Single-layer membrane valves for elastomeric microfluidic devices

A. R. Abate and D. A. Weitz[a)]
Department of Physics School of Engineering and Applied Sciences, Harvard University, Cambridge, Massachusetts 02138, USA

(Received 18 March 2008; accepted 23 May 2008; published online 19 June 2008)

We characterize single-layer membrane valves for elastomeric microfluidic devices. The devices are simple to fabricate using standard single-layer softlithography; moreover, they afford continuous control over flow rate. This combines the simplicity of stamped microfluidic devices with the precision control of membrane valves, which we demonstrate by steering objects in the flow using a simple device. © *2008 American Institute of Physics*. [DOI: 10.1063/1.2945797]

Valves increase the usefulness of microfluidic devices by enabling one active control of flows to switch, isolate, and pump fluids. Many microfluidic valves have been developed[1–7] but membrane valves, in particular, afford superior control.[8–12] However, current membrane valve devices require at least two layers of polydimethylsiloxane (PDMS) and a mask aligner for fabrication, increasing production complexity, and negating the primary advantage of simplicity afforded by stamped PDMS devices. A system that could combine the simplicity of stamped single-layer PDMS devices with the superior flow control of multilayer membrane devices would therefore be very useful; however, such a system has not yet been developed.

In this letter, we present a method that combines the simplicity of stamped single-layer PDMS devices with the precision control of membrane valves. We produce membrane valve devices that exist entirely in a single plane, enabling them to be fabricated in a single stamp using standard single-layer softlithography.[13–15] The valves have a fast response time and can be used to continuously control flow rate. To characterize this control, we measure the pressure drop and flow rate along microchannels as a function of valve actuation pressure. In addition, to optimize the valves, we vary key design parameters, such as valve length and channel aspect ratio, and monitor the valve performance. We show that high aspect ratio devices fabricated in soft PDMS are optimal and use these valves to steer droplets in a flow.

Membrane valves consist of a flexible elastomeric membrane separating two microchannels. An example of a single-layer membrane valve is shown in Fig. 1(a). The valve is actuated by pressurizing the control channel, which is the channel shaped like an upsidedown "T" in the diagram. Actuation deflects the PDMS membrane, which constricts the neighboring fluid channel, as shown in the upper-left corner of Fig. 1(c). In multilayer membrane valve devices, the control channels are above the fluid channels, existing in a separate layer of PDMS, and requiring two-step fabrication and alignment. In single-layer membrane valve devices, the control and fluid channels exist in the same layer, as shown in Figs. 1(a)–1(c). This simple architectural difference is the source of a significant advantage. Because the valves and channels exist in the same plane, the entire microfluidic device can be fabricated in a single stamp.

To quantify the control afforded by single-layer valves, we measure the pressure drop in the constricted channel as a function of the actuation pressure applied to the valve channel. To measure the actuation pressure, we exploit the inherent elasticity of the PDMS. We apply fixed input pressure to the fluid channel while varying actuation pressure of the valve channel. This deflects the elastic PDMS membrane, which we optically measure by tracking the wall in R_1, as shown in Figs. 1(b) and 1(c). This provides measurements of the wall deflection as a function of the actuation pressure, which we use to calibrate the device. To extract a smooth calibration curve, we fit the data to a line, as shown in Fig. 1(d). The calibration enables us to infer the pressure used to actuate the valve from the optically measured deflection of the PDMS membrane.

To measure the pressure drop across the constricted fluid channel, we make use of a microfluidic differential manometer.[16,17] A differential manometer is a simple device consisting of a measurement channel and a comparator

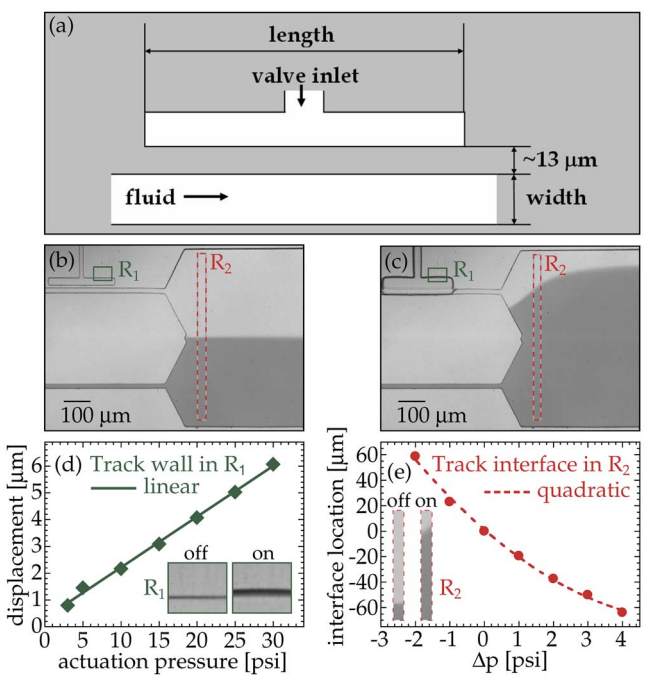

FIG. 1. (Color online) (a) Single-layer valve as seen from above with design parameters labelled. (b) Differential manometer used to measure pressure drop across the upper channel. When the valve is not actuated the fluid interface forms in the middle of the basin. (c) When the valve is actuated the interface forms higher up. (d) Calibration data of wall deflection in R_1 as a function of valve actuation pressure and (e) interface location in R_2 as a function of pressure difference between the upper and lower channels.

[a)]Electronic mail: weitz@seas.harvard.edu.

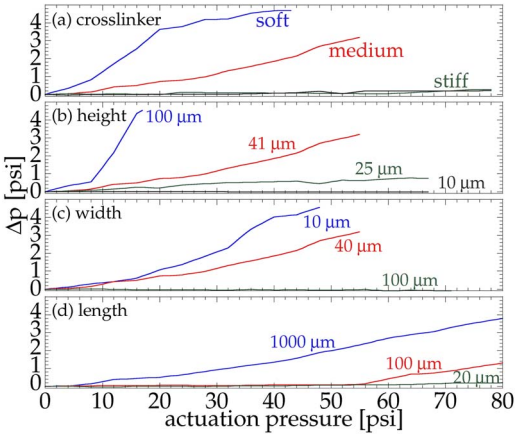

FIG. 2. (Color online) Pressure drop across the constricted channel as a function of the valve actuation pressure. Maximum pressure drop is 5 psi. (a) Effects of varying cross-linker concentration: width=40 μm, length =400 μm, height=41 μm, blue=6.3%, red=7.7%, green=9.1%, gray =11.8%. (b) Effects of varying channel height: width=40 μm, length =400 μm, cross-linker=7.7%. (c) Effects of varying channel width: length=400 m, height=41 μm, cross-linker=7.7%. (d) Effects of varying valve head length: width=40 μm, height=41 μm, cross-linker=7.7%.

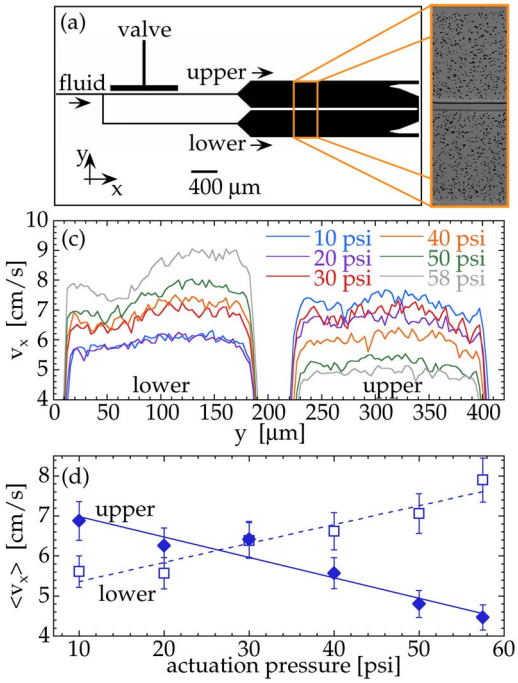

FIG. 3. (Color online) Continuous flow control device. Total flow rate is 1000 μl/h. (a) Schematic of the device with axis definitions. (b) Enhanced image of the flowing tracer particles. (c) Flow profiles measured using PIV. (d) Average flow speeds for the upper and lower channels as a function of valve actuation pressure.

channel. The two channels empty into a large basin channel, as shown in Figs. 1(b) and 1(c). Dyed and undyed miscible fluids are pumped through the channels at an equal pressure of 5 psi. Because the flows are laminar, a sharp interface forms in the basin channel where the pressures of the fluids are equal. When the valve is not actuated, the interface forms at the geometrical center of the basin, as shown in Fig. 1(b). By contrast, when the valve is actuated, the pressure of the clear fluid, which has moved through the constricted measurement channel, is lower than that of the dyed fluid, which has moved through the unconstricted comparator channel, and the interface moves upwards to compensate, as shown in Fig. 1(c) and in the movie available online.[18] After calibration,[18] the location of the interface in R_2 affords a measurement of the pressure drop Δp along the measurement channel, as shown by the calibration data in Fig. 1(e).[17] The optical measurements of the membrane deflection and the interface location afford simultaneous measurements of the valve actuation pressure and the measurement channel pressure drop, which we use to quantify valve performance.

The performance of a valve depends on its physical properties, which can be understood from the approximation for pressure driven laminar flow in a high aspect ratio channel, $\Delta p \propto vl/w^3h$, where Δp is the pressure drop along a microchannel, v is fluid flow rate, l is channel length, w is channel width, and h is channel height, with $w \ll h$. The approximation highlights the key properties of channel cross-sectional area and aspect ratio. Membrane valves control flow by constricting microchannels and regulating their hydrodynamic resistance. To determine the importance of the flexibility of the PDMS membrane, we vary cross-linker concentration for fixed cure time of 90 min.[19] Performance curves for devices with different PDMS stiffness are shown in Fig. 2(a). The curves for soft devices are steeper than for stiff devices, demonstrating that soft devices afford larger pressure drop and greater control. The pressure drop across a channel also depends on its aspect ratio, which we vary by independently varying channel width [Fig. 2(b)] and channel height [Fig. 2(c)]. In both cases, performance curves for high aspect ratio channels are steeper than for low aspect ratio channels, demonstrating that high-aspect ratio channels afford greater control. Pressure drop also depends on the length of the channel constriction, which we vary by varying the length of the valve, as shown in Fig. 1(a). Performance curves for long valves are steeper than for short valves, demonstrating that long valves afford greater control. Thus, high aspect ratio channels and long valves fabricated in soft PDMS are optimal and for full valve actuation, seal off the fluid channel. Other microfluidic components can be placed 50 μm away from the control channels without being deformed by the valve actuation.

To quantify the range and precision of flow rate control afforded by single-layer valves, we fabricate a device consisting of two parallel channels branching from a single channel. The flow rates along the branching paths can be controlled using a valve, as shown in Fig. 3(a). We fix the total flow rate through the device at 1000 μl/h using a syringe pump. When the valve is actuated, the flow rate in the upper channel is reduced while the flow rate in the lower channel is increased. We measure the velocity profiles for a sequence of actuation pressures using particle imaging velocimetry (PIV). For the PIV, we image 1 μm polystyrene tracer particles at the vertical center of the channels using a 40× objective with a 2 μm depth of field. An example enhanced image of the flowing particles is shown in Fig. 3(b). The velocity profiles are pluglike due to the low aspect ratio of the channels, as shown in Fig. 3(c). To determine whether this flow control is continuous, we calculate the average flow speeds by integrating the profiles, and plot them as a function of actuation pressure [Fig. 3(d)]. The flow speeds are roughly linear versus actuation pressure, demonstrating continuous flow rate control. Moreover, this control has a fast response time; whereas flow changes can take minutes to stabilize

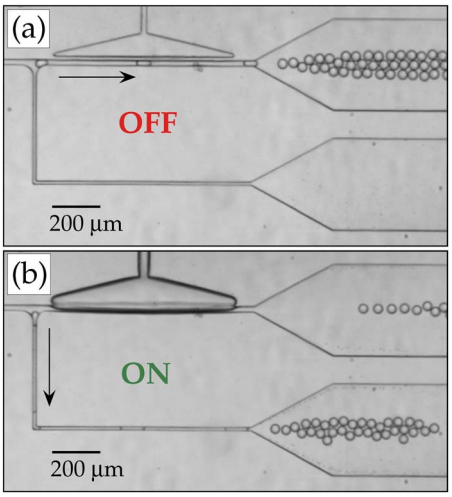

FIG. 4. (Color online) Membrane valve steering device. Droplet production flow rates are 10 μl/h inner water phase and 100 μl/h outer oil phase. (a) When the valve is not actuated, drops go into the upper channel. (b) When the valve is actuated, drops are forced to go into the lower channel.

using a syringe pump, flow rate can be changed in ~5 ms using a single-layer membrane valve.

The precision control afforded by single-layer valves enables drops to be steered in a microfluidic device. Together with a detector and automated valve actuator, this can be used for the important function of sorting. As a simple demonstration, we steer emulsion drops using the single-layer valves.[18] To create the drops, we use a flow-focus drop maker. Each 20 μm drop is a discreet object that follows the path of least hydrodynamic resistance; thus, when the valve is not actuated, the drops go into the upper waste channel [Fig. 4(a)]. By contrast, when the valve is actuated, the increased hydrodynamic resistance of the upper path forces drops into the lower collection channel, as shown in Fig. 4(b), and in the movie online.[18]

Single-layer membrane valves afford continuous, fast response time flow rate control, making them suitable for applications such as microfluidic sorting and droplet synchronization. Moreover, because the devices exist in a single plane, they can be made in a single stamp using single-layer soft lithography. They combine the precision control afforded by membrane valves with the simple fabrication of single-layer PDMS devices.

We thank Jeremy Agresti, Enric Santanach-Carreras, and Howard Stone for their help. This work was supported by the NSF (DMR-0602684 and DBI-0649865), the Harvard MR-SEC (DMR-0213805).

[1]C. R. Neagua, J. G. E. Gardeniersaand, M. Elwenspoeka, and J. J. Kellyb, Electrochim. Acta **42**, 3367 (1997).
[2]Q. Yu, J. M. Bauer, J. S. Moore, and D. J. Beebe, Appl. Phys. Lett. **78**, 2589 (2001).
[3]A. Terray, J. Oakey, and D. W. M. Marr, Science **296**, 1841 (2002).
[4]S. Lee, W. Jeong, and D. J. Beebe, Lab Chip **3**, 164 (2003).
[5]H. Takaoa, K. Miyamurab, H. Ebib, M. Ashikia, K. Sawadaa, and M. Ishidaa, Sens. Actuators, A **2**, 468 (2005).
[6]T. Pan, S. J. McDonald, E. M. Kai, and B. Ziaie, J. Micromech. Microeng. **15**, 1021 (2005).
[7]M. J. Fuerstman, P. Garstecki, and G. M. Whitesides, Science **315**, 828 (2007).
[8]M. A. Unger, H.-P. Chou, T. Thorsen, A. Scherer, and S. R. Quake, Science **288**, 113 (2000).
[9]T. Thorsen, S. J. Maerkl, and S. R. Quake, Science **298**, 580 (2002).
[10]J. Liu, M. Enzelberger, and S. Quake, Electrophoresis **23**, 1531 (2002).
[11]J. Hong, V. Studer, G. Hang, W. Anderson, and S. Quake, Nat. Biotechnol. **22**, 435 (2004).
[12]C. Hansen, S. Classen, J. Berger, and S. Quake, J. Am. Chem. Soc. **128**, 3142 (2006).
[13]N. Sundararajan, D. Kim, and A. A. Berlin, Lab Chip **5**, 350 (2005).
[14]C.-H. Lee, S.-K. Hsiung, and G.-B. Lee, J. Micromech. Microeng. **17**, 11211129 (2007).
[15]G. M. Whitesides, Nature (London) **442**, 368 (2006).
[16]A. Groisman, M. Enzelberger, and S. R. Quake, Science **300**, 955 (2003).
[17]M. Abkarian, M. Faivre, and H. A. Stone, Proc. Natl. Acad. Sci. U.S.A. **103**, 538 (2006).
[18]See EPAPS Document No. E-APPLAB-92-091824 for a detailed discussion of the device fabrication and measurement procedures. For more information on EPAPS, see http://www.aip.org/pubservs/epaps.html.
[19]X. Q. Brown, K. Ookawa, and J. Y. Wong, Biomaterials **26**, 3123 (2005).